



# Torsion sensor based on inter-core mode coupling in seven-core fiber

FENGZE TAN,<sup>1</sup> ZHENGYONG LIU,<sup>2,4</sup> JIAJING TU,<sup>1,3</sup> CHANGYUAN YU,<sup>1,5</sup>  
CHAO LU,<sup>1</sup> AND HWA-YAW TAM<sup>2</sup>

<sup>1</sup>Photonics Research Center, Department of Electronic and Information Engineering, The Hong Kong Polytechnic University, Hong Kong, China

<sup>2</sup>Photonics Research Center, Department of Electrical Engineering, The Hong Kong Polytechnic University, Hong Kong, China

<sup>3</sup>Beijing Engineering and Technology Center for Convergence Networks and Ubiquitous Services, University of Science and Technology Beijing, Beijing 100083, China

<sup>4</sup>zhengyong.liu@connect.polyu.hk

<sup>5</sup>changyuan.yu@polyu.edu.hk

**Abstract:** We proposed a novel torsion sensor based on inter-core mode coupling in seven-core fiber (SCF). The torsion sensor is fabricated by tapering a commercially available SCF spliced with two single mode fibers. Waist diameter and length of the taper structure were experimentally optimized to achieve good transmission spectrum. Based on this structure, the torsion measurement was conducted, and the experimental results demonstrated that the transmission spectrum shows a red shift with the fiber twist. The torsion sensitivity increases with the twisting angle, which can achieve as high as 1.00 nm/°. The direction of wavelength shift was observed to be opposite when twisting the tapered SCF in clockwise and counter-clockwise direction, demonstrating its capability to discriminate the rotation orientation. Moreover, all the measurements were repeated in attempts to confirm its stable performance as well as high accuracy. Mode coupling dynamics and theory of optical anisotropy in twisted fiber are adopted to discuss the sensitivity performance, which agrees well with experimental results. The novel torsion sensor could provide a promising candidate for the applications requiring accurate rotation.

© 2018 Optical Society of America under the terms of the [OSA Open Access Publishing Agreement](#)

**OCIS codes:** (060.2310) Fiber optics; (060.2370) Fiber optics sensors.

## References and links

1. R. Xu, A. Yurkewich, and R. V. Patel, "Curvature, Torsion, and Force Sensing in Continuum Robots Using Helically Wrapped FBG Sensors," *IEEE Robotics and Automation Letters* **1**(2), 1052–1059 (2016).
2. M. Kristensen, L. Nielsen, and L. Glavind, "A Multicore Fiber Sensor for Monitoring Twists of Wind Turbine Parts," In *Bragg Gratings, Photosensitivity, and Poling in Glass Waveguides*. 2016 OSA Technical Digest Series (Optical Society of America, 2016), paper BM5B–6.
3. X. Dong, Z. Xie, Y. Song, K. Yin, Z. Luo, J. Duan, and C. Wang, "Highly sensitive torsion sensor based on long period fiber grating fabricated by femtosecond laser pulses," *Opt. Laser Technol.* **97**(2), 248–253 (2017).
4. B. Huang and X. Shu, "Highly sensitive torsion sensor with femtosecond laser-induced low birefringence single-mode fiber based Sagnac interferometer," *Opt. Express* **26**(4), 4563–4571 (2018).
5. H. Zhang, Z. Wu, P. P. Shum, X. Shao, R. Wang, X. Q. Dinh, S. Fu, W. Tong, and M. Tang, "Directional torsion and temperature discrimination based on a multicore fiber with a helical structure," *Opt. Express* **26**(1), 544–551 (2018).
6. T. Kobayashi, M. Nakamura, F. Hamaoka, K. Shibahara, T. Mizuno, A. Sano, H. Kawakami, A. Isoda, M. Nagatani, H. Yamazaki, Y. Miyamoto, Y. Amma, Y. Sasaki, K. Takenaga, K. Aikawa, K. Saitoh, and Y. Jung. D. J. Richardson, K. Pulverer, M. Bohn, M. Nooruzzaman, and T. Morioka, "1-Pb/s (32 SDM/46 WDM/768 Gb/s) C-band Dense SDM Transmission over 205.6-km Single-mode Heterogeneous Multi-core Fiber using 96-Gbaud PDM-16QAM Channels", in *Optical Fiber Communication Conference*, 2017 OSA Technical Digest Series (Optical Society of America, 2017), paper Th5B.1.
7. K. Shibahara, T. Mizuno, L. Doowhan, Y. Miyamoto, H. Ono, and K. Nakajima, "DMD-Unmanaged Long-Haul SDM Transmission Over Employing Intermodal Interference Cancelling Technique," in *Optical Fiber Communication Conference*, **Vol.1** of 2017 OSA Technical Digest Series (Optical Society of America, 2017), paper Th4C.6.

8. K. Pulverer, *et al.*, "First Demonstration of Single-Mode MCF Transport Network with Crosstalk-Aware In-Service Optical Channel Control," in *European Conference and Exhibition on Optical Communication*, pp. 1–3, September 2017.
9. E. Burrows, N. K. Fontaine, and H. Chen, "Long-Distance Transmission over Coupled-Core Multicore Fiber," in *European Conference and Exhibition on Optical Communication*, pp. 40–42, 2016.
10. T. Sakamoto, *et al.*, "High Spatial Density Six-mode Seven-core Fibre for Repeated Dense SDM Transmission," in *European Conference and Exhibition on Optical Communication*, pp. 1–3, September 2017.
11. J. M. D. Mendinueta, *et al.*, "Experimental Demonstration of a 53 Tb/s Coherent SDM-TDM Add/Drop/Through Optical Network with Time-division Spatial Super-channels and High-speed Joint Switching System," in *European Conference and Exhibition on Optical Communication*, pp. 1–3, September 2017.
12. A. S. Kurkov, S. A. Babin, I. A. Lobach, and S. I. Kablukov, "New mechanism of the mode coupling in multi-core fiber lasers," *33*(1), 68761Q (2008).
13. Y. Huo, G. G. King, and P. K. Cheo, "Second Harmonic Generation using a High-Energy and Tunable Q-switched Multicore Fiber Laser," *IEEE Photonics Technol. Lett.* **16**(10), 2224–2226 (2004).
14. J. E. Antonio-Lopez, Z. S. Eznavch, P. LiKamWa, A. Schülzgen, and R. Amezcua-Correa, "Multicore fiber sensor for high-temperature applications up to 1000°C," *Opt. Lett.* **39**(15), 4309–4312 (2014).
15. J. Villatoro, O. Arrizabalaga, G. Durana, I. Sáez de Ocariz, E. Antonio-Lopez, J. Zubia, A. Schülzgen, and R. Amezcua-Correa, "Accurate strain sensing based on super-mode interference in strongly coupled multi-core optical fibres," *Sci. Rep.* **7**(1), 4451 (2017).
16. J. P. Moore and M. D. Rogge, "Shape sensing using multi-core fiber optic cable and parametric curve solutions," *Opt. Express* **20**(3), 2967–2973 (2012).
17. P. S. Westbrook, T. Kremp, K. S. Feder, W. Ko, E. M. Monberg, H. Wu, D. A. Simoff, T. F. Taunay, and R. M. Ortiz, "Continuous Multicore Optical Fiber Grating Arrays for Distributed Sensing Applications," *J. Lightwave Technol.* **35**(6), 1248–1252 (2017).
18. M. S. Yoon, S. B. Lee, and Y. G. Han, "In-line interferometer based on intermodal coupling of a multicore fiber," *Opt. Express* **23**(14), 18316–18322 (2015).
19. F. Y. M. Chan, A. P. T. Lau, and H.-Y. Tam, "Mode coupling dynamics and communication strategies for multi-core fiber systems," *Opt. Express* **20**(4), 4548–4563 (2012).
20. J. Zubia, J. Arrue, and A. Mendioroz, "Theoretical analysis of the torsion-induced optical effect in a plastic optical fiber," *Opt. Fiber Technol.* **3**(2), 162–167 (1997).
21. J. Tu, K. Saitoh, M. Koshiha, K. Takenaga, and S. Matsuo, "Design and analysis of large-effective-area heterogeneous trench-assisted multi-core fiber," *Opt. Express* **20**(14), 15157–15170 (2012).
22. S. Yin, P. B. Ruffin, and F. T. S. Yu, *Fiber Optic Sensors, Second Edition*, (CRC Press, 2008).
23. W. Yiping, M. Wang, and X. Huang, "In fiber Bragg grating twist sensor based on analysis of polarization dependent loss," *Opt. Express* **21**(10), 11913–11920 (2013).
24. O. Frazão, R. M. Silva, J. Kobelke, and K. Schuster, "Temperature- and strain-independent torsion sensor using a fiber loop mirror based on suspended twin-core fiber," *Opt. Lett.* **35**(16), 2777–2779 (2010).

## 1. Introduction

Owing to the intrinsic advantages, such as compact size, low-cost, and immunity to electromagnetic interference, fiber optic sensors have attracted extensive interests and various fiber optic sensors are designed and fabricated according to different measurements. Torsion, one of the important mechanical parameters, has become significant due to its potential applications in the areas of robotics and civil engineering. For example, in needle-based continuum robots for surgical interventions, shape sensors enable the flexible needles to steer through soft tissue so that the cable-driven robot can be positioned accurately. However, during needle steering and tissue manipulation tasks, the applied torsion may disorientate the tool tip and then affect the accuracy of 3D shape reconstruction [1]. Therefore, a needle-sized optical fiber torsion sensor with high sensitivity is urgent and potential in continuum robots. Apart from that, structural monitoring of wind turbines blades became necessary for detection of fatigue failure as well as production optimization of wind turbines. The monitoring can be realized by measuring the twist of wind turbines and fiber-optic sensor was utilized at the first attempt [2]. However, the resolution achieved is nonuniform and the sensitivity is very slow. In order to implement torsion sensor with high sensitivity, various specialty optical fibers or structures have been utilized. Long period grating (LPG) inscribed on single mode fiber using femtosecond laser was demonstrated to be highly sensitive torsion sensor and X. Dong *et al* reported that the different resonant wavelengths of LPG, corresponding to various orders of the modes, show different shifts, in which LP<sub>04</sub> resonance wavelength reaches the highest sensitivity of 31.6 pm/(rad/m) [3]. Another highly sensitive torsion sensor was proposed and

demonstrated experimentally based on Sagnac interferometer (SI) constructed by a SMF with low birefringence induced by a femtosecond laser. This torsion sensor exhibits a sensitivity of up to  $3.25 \text{ nm}/^\circ$  [4], which is the highest one for the SI based torsion sensors reported so far. In addition, Multicore fiber (MCF) with pre-twisted long helical structure as well as Multimode fiber (MMF) spliced on both ends was recently reported to be sensitive to torsion angle and the sensitivity can achieve about  $0.118 \text{ nm}/(\text{rad}/\text{m})$  [5]. However, these torsion sensors with high sensitivity are based on the custom-made specialty optical fibers or sophisticated structures, which are inevitably costly and time-consuming.

In order to cope with the increasing need of the internet capacity, space-division multiplexing technique using multicore fibers has been investigated extensively in recent years [6–9], in which Seven-core fiber (SCF) shows its prospect on future application as one typical multicore fiber [10,11]. Apart from the applications for communication, multicore fiber has attracted a lot of attentions in the area of optical fiber laser and sensors. The isometrically arranged cores in multicore fibers enable the light power to transfer to each other, which generates the in-phase supermodes to achieve high beam quality in fiber lasers. A SCF-laser with good beam quality was demonstrated and later was used for second harmonic generation [12,13]. Meanwhile, the strong coupling of multicore fiber in which the cores are close enough to form supermodes is demonstrated to be promising for high temperature measurement [14] and accurate strain sensing [15]. For shape sensing, Jason P. Moore realized complex three-dimensional fiber shape sensing by using tri-core fibers with distributed Fiber Bragg Gratings (FBGs). A set of Frenet-Serret equations were numerically solved to convert distributed curvature measurement into three-dimensional shape [16]. In addition, twisted SCF with long continuous fiber grating sensor arrays can be utilized for shape sensing. In this scheme, grating in outer cores and helical twist structure in SCF were respectively sensitive to local bend and twist, which contributes to precise shape reconstruction [17].

In this paper, we demonstrated a novel torsion sensor based on the inter-core mode coupling effect occurring in SCF. The fiber torsion sensor was fabricated by tapering a SCF, which is then spliced to the conventional single mode fibers (SMF) on both ends. The core of SMF was aligned to the center core of SCF. Owing to the reduced distance between cores, the inter-core mode coupling in the tapered fiber was enhanced, which is highly depending on the torsion applied to the taper waist. The experimental results show that the torsion sensitivity increases with the fiber twist, meaning that the response can be easily tuned by setting proper pre-twist angle in practice. In the meantime, the rotation direction can be discriminated by monitoring the red or blue shift of the spectrum. Furthermore, repeatable measurements based on various batches of sensors but with identical dimensions show the similar performance in terms of sensitivity and accuracy, signifying the good repeatability of the torsion sensor. The experimental findings are explained theoretically in the end by adopting mode coupling dynamics and theory of optical anisotropy in twisted fiber. This optical fiber torsion sensor can find potential applications in civil and mechanical engineering.

## 2. Fabrication of optical fiber torsion sensor

The fiber torsion sensor was realized by splicing two single-mode fibers to a section of tapered SCF on both ends. A  $\text{CO}_2$  laser glass-processing machine (Fujikura, LZM-100) is utilized to taper the SCF, a trench assisted multicore fiber from YOFC in China. Figure 1 shows the schematic drawing of the setup and the inset is the cross section of the SCF. Its cladding diameter, core diameter and core pitch size are  $150 \text{ }\mu\text{m}$ ,  $8 \text{ }\mu\text{m}$  and  $42 \text{ }\mu\text{m}$ , respectively. A taper structure is fabricated so as to strengthen the coupling between center core and outer cores due to the smaller pitch size. Both the laser power and motors are controlled by program. Thus, we can fabricate taper structure on SCF precisely with different dimensions to obtain desirable spectrum. Typically, the deviation between the actual and designed taper is less than  $5 \text{ }\mu\text{m}$ .

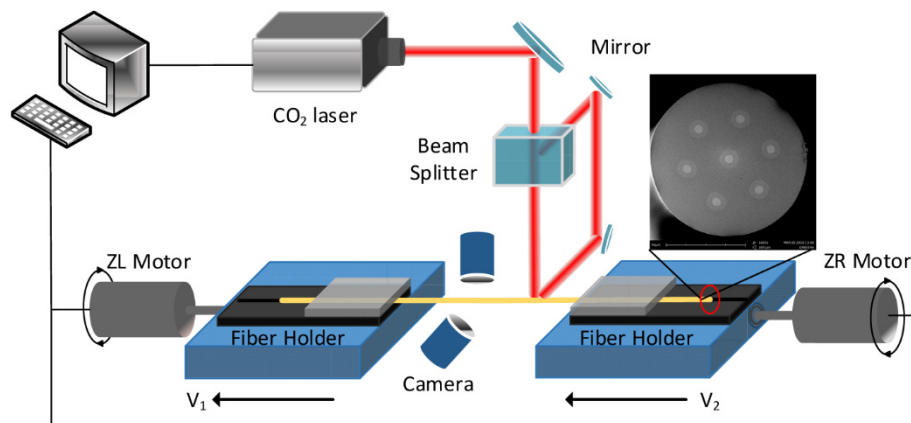


Fig. 1. Schematic drawing of the setup to taper the seven-core fiber using CO<sub>2</sub> laser.

Since the core pitch becomes smaller after the SCF is tapered, the coupling between the center core and outer cores can be enhanced, leading to obvious oscillation in the transmission spectrum. To verify this, an optical spectrum analyzer (OSA, Yokogawa AQ6370) and a Broadband Light Source (BLS) ranging from 1250 nm to 1650 nm were used to observe the transmission spectrum. Since the mode coupling is highly dependent on the taper dimension, including waist diameter, length and transition length [18], sensor samples with different taper dimensions were investigated in order to achieve optimized taper structure. We set the transition length as 5 mm and discuss the influence of waist diameter and length on the spectra. Figure 2(a) and 2(b) plot the spectra of the sensor with different waist diameters and lengths, respectively. Observed from the results, the spectral extinction ratio increases when reducing the waist diameter, and the fringe spacing decreases with the increase of waist length. In perspective of practical use, smaller waist diameter weakens the strength of the taper, therefore, the waist diameter is chosen as 30  $\mu\text{m}$  for later torsion measurement. The waist length is set to be 5 mm.

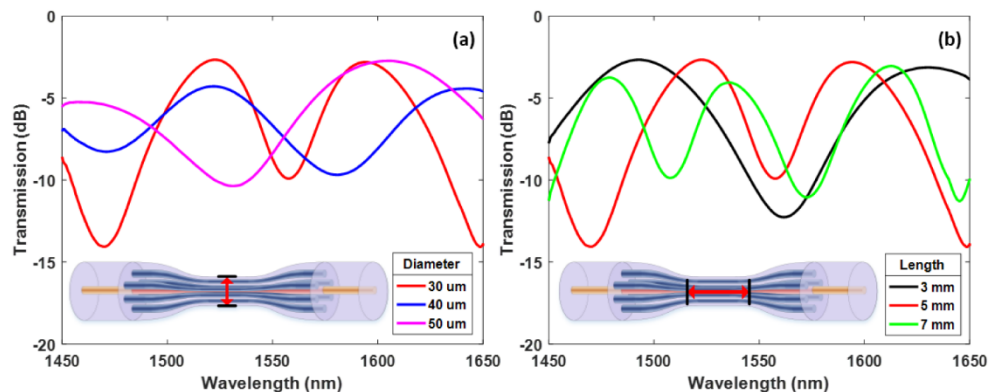


Fig. 2. Transmission spectra of the torsion sensors with different (a) waist diameters and (b) waist lengths.

### 3. Experiment and results

The experimental setup to measure the torsion based on tapered SCF is shown in Fig. 3. Same OSA and BLS were utilized to monitor the spectrum. The tapered SCF was fixed on two holders, one of which can be rotated axially with a precision of 0.1°. Accurate alignment between the two holders was conducted to avoid any radial displacement during twisting. In experiment, we initially placed two sections of SCF on the holders to do the alignment and

then fixed the holders so that the offset error can be limited within just a few micrometers. The twisting length between two holders was set to be 30 mm in order to cover the whole taper region. The right-side holder was rotated precisely in clockwise and counter-clockwise direction.

In the torsion sensing experiment, fiber twist angle varied from  $0^\circ$  to  $900^\circ$  with a step of  $20^\circ$  and the corresponding spectrum at each angle was recorded. The spectral resolution of the OSA is 0.05 nm. One valley in the spectrum was chosen to trace the wavelength change with torsion and the result is illustrated in Fig. 4, the inset of which plots the spectrum shift when twisting the tapered SCF from  $0^\circ$  to  $360^\circ$ . From the results, the transmission spectrum shows red shift with the increase of torsion angle. In addition, the wavelength shift increases nonlinearly with the fiber twist, which means that the sensitivity of torsion sensor increases during the fiber twist.

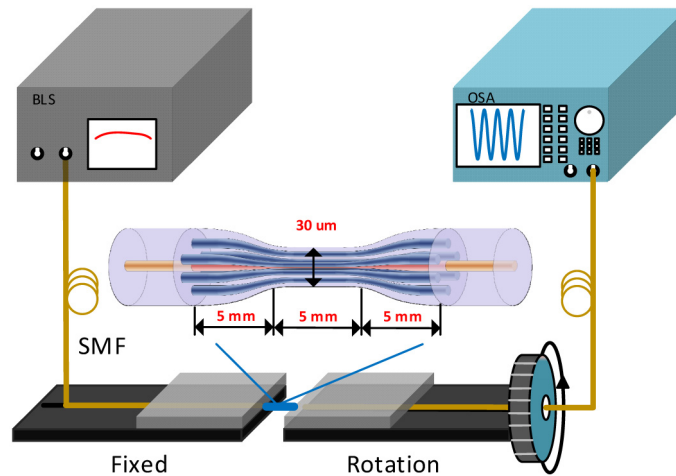


Fig. 3. Experimental setup to measure the torsion angle based on tapered SCF.

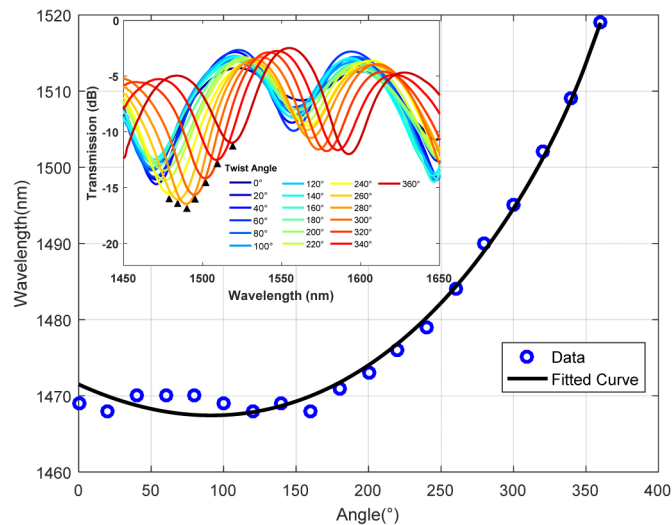


Fig. 4. Experimental results of the torsion angle measurement, including spectrum shift under twisting angle from  $0^\circ$  to  $360^\circ$  and corresponding wavelength shift.



### 3.1 Tunable sensitivity

Since the response of the torsion sensor is not linear, the sensitivity changes with the twisting angle. However, relatively linear response can be obtained in short twisting range within  $90^\circ$ . The tunable torsion sensitivity is characterized by pre-twisting the tapered SCF to different angles, and the spectra of three measurement ranges with pre-twisting angle of  $160^\circ$ ,  $360^\circ$ , and  $560^\circ$  are plotted in Figs. 5(a)-5(c), respectively. From the results, we can see that with the same twisting angle increase of  $60^\circ$ , the range with larger pre-twisting angle shows wider wavelength shift. Figure 6 shows the torsion sensitivities in seven measurement ranges with various pre-twisting angles, and the sensitivity can achieve as high as  $1.00 \text{ nm}/^\circ$ . Therefore, the sensitivity of the torsion sensor realized by the tapered SCF can be easily tuned by introducing a proper pre-twisting angle.

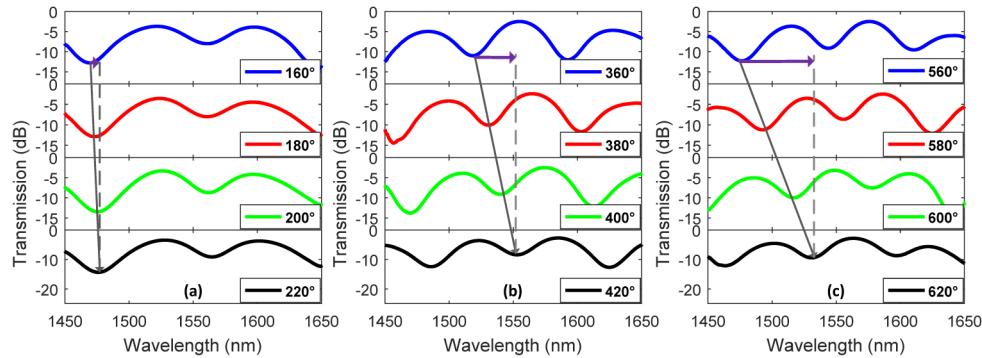


Fig. 5. Wavelength shift in transmission spectra when the sensor is rotated at a step of  $20^\circ$  in three measurement ranges with pre-twisting angle of: (a)  $160^\circ$ , (b)  $360^\circ$ , and (c)  $560^\circ$ .

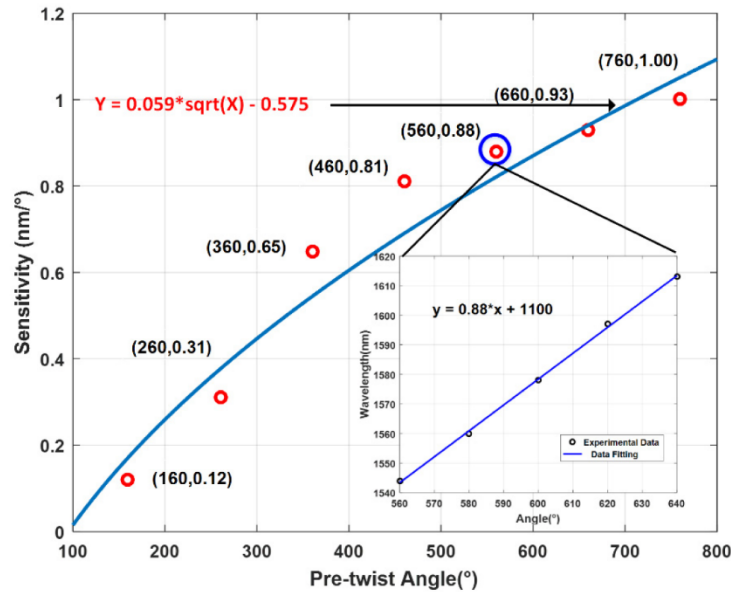


Fig. 6. Torsion sensitivity of the torsion sensor based on tapered SCF in measurement ranges with different pre-twisting angles.

### 3.2 Discrimination of twisting direction

To investigate the ability to discriminate the rotation direction, the tapered SCF was pre-twisted to  $360^\circ$  and rotated in clockwise (C.W.) and counter-clockwise (C.C.W.) direction.

The taper still follows the same dimension shown in Fig. 3. Figure 7 plots the measured wavelength shift when twisting the sensor from  $360^\circ$  to  $540^\circ$  in clockwise direction and  $360^\circ$  to  $180^\circ$  in counter-clockwise direction, corresponding to  $2\pi$  in total. As illustrated from the results, the twisting direction can be distinguished easily by monitoring the blue or red shift of the spectrum, even though larger wavelength shift is observed in clockwise direction due to the nonlinear response.

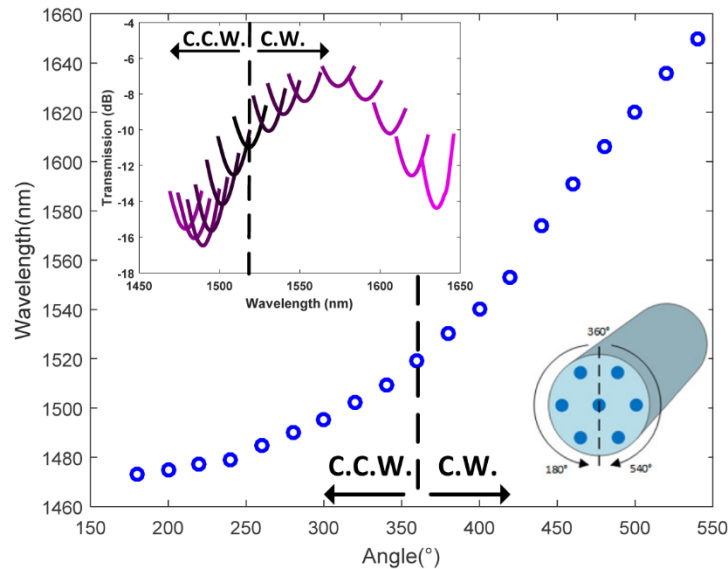


Fig. 7. Measured wavelength shifts with respect to the torsion in C.W. and C.C.W. direction using the tapered SCF with a pre-twisting angle of  $360^\circ$ .

### 3.3 Repeatability

In the experiments, the torsion measurements were repeated to estimate the accuracy by fabricating three torsion sensors with the same dimension and by measuring the torsion three times using one torsion sensor. Three sensors were fabricated by tapering the SCF into  $30\ \mu\text{m}$  in diameter and the waist length as well as up/down-tapering lengths are 5 mm. Torsion response for each sensor was characterized to show the fabrication repeatability. The results are shown in Fig. 8(a), and good agreement is achieved for the three batches of the sensors. This indicates that the performance of the torsion sensor based on tapered-SCF can be easily repeated if the sensor dimension is kept the same, which is of great importance in the perspective of mass production. Figure 8(b) demonstrates the measured wavelength shift with respect to the torsion of three measurements using the same sensor. Both the largest errors in terms of wavelength shift are 2 nm, meaning that the torsion sensor has a measurement accuracy of about  $\pm 1^\circ$  if taking the sensitivity of  $0.85\ \text{nm}/^\circ$  into account.

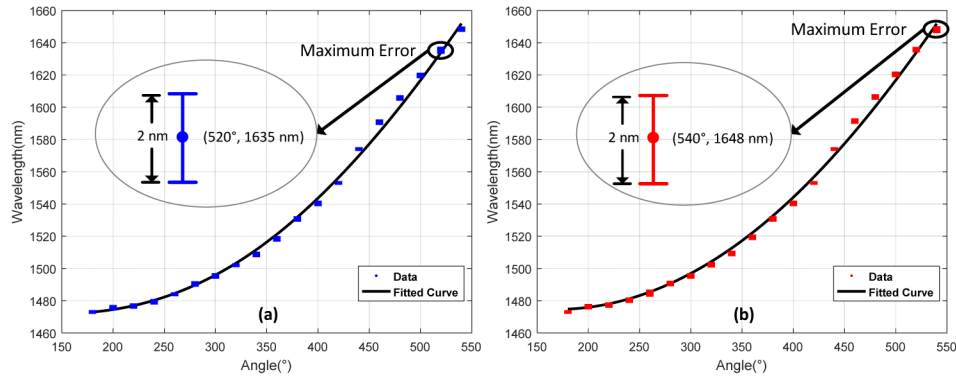


Fig. 8. Torsion measurement results achieved by (a) using three torsion sensors with the same taper dimension, and (b) repeating the torsion measurement using one sensor.

#### 4. Discussion

According to the mode coupling dynamics in SCF with identical seven cores [19], the mode amplitude in each core at propagation distance  $z$  can be obtained when light is launched into the center core. The output normalized mode power in center core can be expressed by:

$$I(z) = \frac{1}{7} + \frac{6}{7} \cos^2(\sqrt{7}Cz), \quad (1)$$

where  $C$  is the mode coupling coefficient between two adjacent cores. The mode coupling coefficient  $C$  is generally dependent on wavelength and RI of cores. In our case, the fiber length is fixed while  $C$  is the variable under investigation. Thus, as for a specific distance  $z$ , the output intensity from the center core has oscillation relationship with respect to wavelength. Any change of refractive index would influence the coupling coefficient and further cause corresponding wavelength shift in the transmission spectrum.

When the SCF is twisted along its longitudinal axis, shearing stress is generated and the stressed region results in RI change. This kind of optical anisotropy is torsion dependent. Stronger torsion induces larger shearing stress. J. Zubia *et al* gave a detailed theoretical analysis of torsion induced optical anisotropy in plastic optical fiber and updated the index ellipsoid [20]. Similar approach is adopted here and the updated RI in polarization state  $\alpha$  and  $\beta$  in a twisted fiber can be expressed as follows:

$$n_{\alpha} = n_{co} + \Delta q \cdot \theta \cdot r \cdot \mu \cdot n_{cl}^3 / 2L, \quad (2)$$

$$n_{\beta} = n_{co} - \Delta q \cdot \theta \cdot r \cdot \mu \cdot n_{cl}^3 / 2L, \quad (3)$$

where  $n_{co}$  and  $n_{cl}$  are the uniform RIs of fiber core and cladding in the absence of torsion,  $\Delta q$  is the element of stress-optical tensor;  $\mu$  is the shearing stress and  $r$  is the radial distance from the center axis of the fiber;  $\theta$  is the torsion angle and  $L$  is the length of the fiber under twisted.

It can be seen that RI variation increases away from the fiber axis. In the case of twisted SCF, the RI of outer cores shows more change than that in center core. Thus, we assume that outer cores in twisted SCF experienced RI change while center core remain RI unchanged. For inter-core mode coupling, since the index changes along two polarization states are different, the coupling between the center core and outer cores is calculated separately. Based on the orthogonality of two polarization states, the output intensity is then the sum of the intensities in two polarization states. Thus, the output intensity in center core can be obtained as:



$$I(z) = I_\alpha(z) + I_\beta(z) = \frac{2}{7} + \frac{6}{7} [\cos^2(\sqrt{7}C_\alpha z) + \cos^2(\sqrt{7}C_\beta z)] \approx \frac{6}{7} \cos[\sqrt{7}(C_\alpha + C_\beta)z] + \frac{8}{7}, \quad (4)$$

where  $C_\alpha$  and  $C_\beta$  are the coupling coefficients between center core with  $n_{co}$  and outer cores with  $n_\alpha$  and  $n_\beta$ . The torsion sensor we proposed is based on SCF with trench assisted, in which the mode coupling has been theoretically analyzed in [21] and the mode coupling coefficient  $C_\alpha$  and  $C_\beta$  can thus be expressed as:

$$C_{\alpha,\beta} = \frac{k(n_{\alpha,\beta}^2 - n_{cl}^2)W_{1-\alpha,\beta}U_{1-q}L_q \sqrt{\frac{\pi a_{1-q}}{2W_{1-q}D}} \exp(-W_{1-q} \frac{D}{a_{1-q}})}{\sqrt{n_{\alpha,\beta}n_q} a_{1-\alpha,\beta} a_{1-q} V_{1-\alpha,\beta} V_{1-q} J_1(U_{1-\alpha,\beta}) J_2(U_{1-q})} \cdot \int_0^{a_{1-\alpha,\beta}} J_0(U_{1-\alpha,\beta} \frac{r}{a_{1-\alpha,\beta}}) I_0[(\frac{W_{1-q}}{a_{1-q}} - \frac{P_2 - P_1 + Y_2 - Y_1}{D - r})r] \exp[\frac{(P_2 - P_1 + Y_2 - Y_1)D}{D - r}] r dr, \quad (5)$$

where  $k$  is the wave number;  $D$  is the pitch size;  $P$  and  $Y$  are the parameters relevant to the ratio between core diameter and pitch size;  $q$  represents the center core. According to the optical anisotropy theory in twisted fiber above, torsion angle variation directly results in the change of  $n_\alpha$  and  $n_\beta$ . Thus, it is acceptable that the coefficient  $C_\alpha$  and  $C_\beta$ , which is directly related to  $n_{\alpha,\beta}$ , can be simplified as  $k \cdot n_{\alpha,\beta}^{3/2}$  in the following analysis on the inter-core mode coupling dependence on torsion angle.

Generally, for torsion measurement, one valley in transmission spectrum was monitored with fiber twist and its corresponding wavelength was traced. For the  $m^{th}$  valley, the wavelength monitored satisfies:

$$[C_\alpha(\lambda_m) + C_\beta(\lambda_m)]z' = (2m+1)\pi, \quad (6)$$

where  $\lambda_m$  denotes the wavelength at the monitored valley and  $z'$  is used to substitute  $\sqrt{7}z$  for simplification in later expressions. Using the simplified mode coupling coefficient, the monitored wavelength  $\lambda_m$  can be expressed as:

$$\lambda_m = \frac{2z'}{2m+1} (n_\alpha^{3/2} + n_\beta^{3/2}), \quad (7)$$

where  $n_\alpha$  and  $n_\beta$  are RIs of two polarization states in outer cores under torsion. To discuss the sensitivity performance, the derivative with respect to  $\theta$  is applied to both sides of Eq. (7), which is formulated by:

$$\frac{d\lambda_m}{d\theta} = \frac{2z'}{2m+1} \cdot \frac{3}{2} (\sqrt{n_\alpha} \frac{dn_\alpha}{d\theta} + \sqrt{n_\beta} \frac{dn_\beta}{d\theta}). \quad (8)$$

Based on Eq. (2) and (3), assuming  $n_\alpha \approx n_\beta$ , the sensitivity can be finally expressed as follows:

$$\frac{d\lambda_m}{d\theta} \approx \frac{3\sqrt{2}z'}{2m+1} (\Delta q \cdot r \cdot \mu \cdot \frac{n_{cl}^3}{2L})^{3/2} \cdot \sqrt{\theta}, \quad (9)$$

where  $z'$ ,  $m$ ,  $\Delta q$ ,  $r$ ,  $\mu$ ,  $L$ ,  $n_{cl}$  are constants with fiber twist. Equation (9) reveals that torsion sensitivity is proportional to the square root of torsion angle and thus increases with fiber twist. Also, it can be intuitively understood that when there comes to the torsion along straight fiber, the twisted region will suffer from high-level tension, which consequently makes the fiber become increasingly sensitive with torsion angle. Moreover, the experimentally achieved sensitivity with respect to the torsion angle is fitted by using Eq. (9),

which shows good agreement as shown in Fig. 6. For the twisted optical fiber cores, we assume the refractive index change induced by torsion to be  $\delta n = 10^{-4}$ - $10^{-5}$ , which also makes sure that  $n_\alpha \approx n_\beta$ . In Eq. (3), the value of refractive index change  $\delta n$  was related to  $\Delta q$ ,  $\theta$ ,  $r$ ,  $\mu$ ,  $L$ ,  $n_{cl}$ . Taking their typical values  $\Delta q \sim 10^{-11}$  m<sup>2</sup>/N,  $r = 42$   $\mu$ m,  $\mu \sim 2 \cdot 10^6$  N/m<sup>2</sup>,  $L = 30$  mm,  $n_{cl} \sim 1.44$  [22], the torsion range turns out to be  $\delta\theta = 200^\circ$ - $2000^\circ$ . Thus, Eq. (9) is theoretically valid for the torsion angle range of  $200^\circ$ - $2000^\circ$ . This also agrees well with the experimental results above. Additionally, the relationships between the measured wavelength and the twisting angle shown in Figs. 4 and 8 are fitted via the integral function of Eq. (9), and as a consequence, both results manifest good agreements.

In summary, our torsion sensor owns tunable sensitivity from 0.12 nm/ $^\circ$  to 1.00 nm/ $^\circ$  within large twist range from  $160^\circ$  to  $940^\circ$  and the ability to discriminate the twist direction with stable performance. In terms of the mechanical strength during practical applications, the sensor can be packaged properly to avoid sharp bending, and in the meantime to ensure only axial twist occurs during the measurement. For current torsion sensors, different operation principles were proposed and various special optical fibers were utilized, such as polarization and fiber loop mirror based on suspended twin-core fiber (TCF). In terms of sensitivity, twist range, mechanical strength and ease of fabrication, of which the levels are determined by the fiber used and fabrication process, the comparison between our torsion sensor and other sensors are shown in Table 1. In addition to the comparable torsion sensitivity with other types, our sensor shows larger measurement range, and in the meantime, it is easy to fabricate with good mechanical strength.

Table 1. Comparison between our torsion sensor and other sensors

Type	Sensitivity	Range	Mechanical strength	Ease of fabrication	Direction Discrimination
Our sensor	0.12-1.00 nm/ $^\circ$	$160^\circ$ - $940^\circ$	High	Easy	Yes
LPG [3]	2.80 nm/ $^\circ$	$0^\circ$ - $160^\circ$	High	Hard	No
SI [4]	3.25 nm/ $^\circ$	$180^\circ$ - $270^\circ$	Medium	Normal	No
Helical MCF [5]	3.90 nm/ $^\circ$	$0^\circ$ - $180^\circ$	Low	Hard	Yes
FBG-PDL [23]	0.955 dB/rad	$0^\circ$ - $180^\circ$	Medium	Normal	-
Suspended-TCF [24]	$1.2 \cdot 10^{-2}$ dB/ $^\circ$	$0^\circ$ - $90^\circ$	Medium	Hard	-

## 5. Conclusion

In this paper, we demonstrated a novel torsion sensor based on the mode coupling between center core and outer cores in a tapered SCF. To obtain desired spectrum for sensing, several torsion sensors were fabricated to optimize the sensor dimension in terms of the taper waist diameter and length. The torsion angle measurements employing this torsion sensor were then conducted in several ranges with different pre-twisting angles. As a result, the sensitivity was observed to increase with fiber twist and achieved as high as 1.00 nm/ $^\circ$ , which is verified as well by the theoretical analysis. The measurement range with higher pre-twisting angle shows larger sensitivity, which allows it to work in desired sensitivity by properly pre-twisting the sensor. Moreover, the clockwise and counter-clockwise twisting can be easily discriminated by monitoring the red/blue shift of the spectrum owing to the monotonic response. Good repeatability to reproduce the torsion sensors using same parameters to conduct the measurements based on them is achieved. The measurement accuracy is estimated to be  $\pm 1^\circ$ . It is easy to fabricate the proposed torsion sensor, which possesses a number of advantages such as robustness, good repeatability and stability, immunity to electromagnetic interference etc., which will be a potential candidate in the applications of structural health monitoring.

## Funding

Hong Kong Polytechnic University (1-ZVHA, 1-ZVGB, 1-BBYE, and 1-BBYS); National Natural Science Foundation of China (NSFC) (61501027); Fundamental Research Funds for the Central Universities (FRF-TP-17-019A2).